Proc. Natl. Acad. Sci. USA
Vol. 78, No. 3, pp. 1416–1420, March 1981
Biochemistry

Contacts between DNA gyrase and its binding site on DNA: Features of symmetry and asymmetry revealed by protection from nucleases

(DNA supercoiling/topoisomerase/enzyme mechanism)

ALAN MORRISON* AND NICHOLAS R. COZZARELLI*†

Departments of *Biochemistry and of †Biophysics and Theoretical Biology, The University of Chicago, Chicago, Illinois 60637

Communicated by Hewson Swift, November 12, 1980

ABSTRACT **DNA gyrase supercoils DNA by passing one DNA segment through another by means of a reversible double-strand break at specific DNA sites. We determined the nucleotide sequence of two highly preferred gyrase binding sites and analyzed the grip of gyrase on the DNA by using protection from nuclease attack. The DNA-breakage site of gyrase was centered in about 50 base pairs (bp) of DNA that was completely protected from DNase I and flanked by DNA regions cut at average intervals of 9.9 bases. The same pattern of protection from DNase I was observed with topoisomerase II′, an enzyme that shares structural homology with gyrase. The gyrase site of DNA breakage was off-center in the 140 bp of DNA protected from exonuclease III digestion. ATP or inhibitors of gyrase had little specific effect on DNase I protection. On addition of a nonhydrolyzable analogue of ATP, previously stable barriers to exonuclease III were invaded and new barriers appeared. We discuss a detailed model uniting these results with previous data on gyrase structure and mechanism.**

The negative supercoiling of DNA is required for *Escherichia coli* DNA replication and fundamentally influences all DNA metabolism (1). DNA gyrase is the enzyme that negatively supercoils DNA (1). Gyrase alters supercoiling in steps of two twists and reversibly catenates and knots closed duplex DNA rings (2–4). These features characterize type 2 topoisomerases, which are widespread in prokaryotic and eukaryotic cells (1, 4). Brown and Cozzarelli (5) explained all of the topoisomerase activities of gyrase by a "sign inversion" mechanism, in which one duplex DNA segment is passed through a transient, double-strand break in another.

The transient phase of DNA breakage by gyrase can be fixed by successive additions of oxolinic acid (Oxo; an inhibitor whose target is gyrase subunit A) and a protein denaturant (6, 7). This cleavage reaction reveals scissions on both strands at points staggered by four base pairs (bp) (8). The resulting termini have a recessed, free 3′ hydroxyl group and a terminal 5′ phosphoryl group attached covalently to a tyrosine residue of gyrase subunit A (8–10). Cleavage occurs with a hierarchy of preferences at similar, asymmetric nucleotide sequences (8, 11). Prominent cleavage sites map the stable gyrase binding sites from which gyrase processively supercoils the DNA (11, 12).

Gyrase prefers to bind and cleave ColE1 DNA at two sites, called "*a*" and "*b*" (11–13). Gyrase bound at the *b* site (but not at the *a* site) requires ATP to cleave efficiently (11–13). Adenyl-5′-yl imidodiphosphate (p[NH]ppA), a nonhydrolyzable analogue of ATP, also stimulates cleavage at the *b* site and, substituted for ATP, leads to negative supercoiling that is stoichiometric with enzyme amount (13). Therefore, it was proposed that ATP binding *per se* provokes a conformational change(s) that is related to DNA double-strand breakage and is sufficient for supercoiling (13).

The publication costs of this article were defrayed in part by page charge payment. This article must therefore be hereby marked "*advertisement*" in accordance with 18 U. S. C. §1734 solely to indicate this fact.

Gyrase protects about 140 bp from micrococcal nuclease digestion and imposes a periodicity of about 10 bp on digestion by DNase I (14). Gyrase also protects positive supertwists from enzymatic relaxation (15). These observations are consistent with the DNA being wrapped in a right-handed supercoil on the outside of gyrase (14).

We used protection from DNases (16) to analyze contacts between gyrase and DNA fragments containing the ColE1 *b* and *a* gyrase sites. The gyrase cleavage site was precisely located within an extensive DNA region bound on the enzyme surface. The nucleases revealed features both of symmetry and asymmetry in the structure of the gyrase·DNA complex. We discuss a model that combines these results, data on gyrase structure, Liu and Wang's image of a nucleosome-like gyrase, and the sign inversion mechanism for DNA supercoiling.

MATERIALS AND METHODS

Labeled DNA Fragments. The ColE1 *Mbo* II E and F fragments, containing the *b* and *a* sites, respectively, were end-labeled by using T4 polynucleotide kinase and [γ-^{32}P]ATP (17). The E and F fragments were cut with *Taq* I and *Hha* I restriction endonucleases, respectively. The resulting 425-bp "*b* fragment" and 350-bp "*a* fragment," labeled only at their right *Mbo* II termini, were purified by polyacrylamide gel electrophoresis. The *b* fragment was labeled only at its left (*Taq* I) end by *Mbo* II digestion of the ^{32}P-labeled ColE1 DNA *Taq* I C fragment. The gyrase cleavage sites are about 125 and 90 bp, respectively, from the right (*Mbo* II) ends of the *b* and *a* fragments.

Enzyme Reactions. Gyrase was reconstituted from purified subunits A and B. Gyrase reactions (5-μl) were with 20 fmol of the [^{32}P]DNA fragment and 50–125 fmol of DNA gyrase in medium containing 35 mM Tris·HCl (pH 7.6), 20 mM KCl, 7 mM potassium phosphate, 5 mM $MgCl_2$, 40 μg of bovine serum albumin per ml, and 0.7 mM dithiothreitol. After 30 min at 30°C, 15 μl of the medium with 0.4 μg of λ phage DNA as competitor was added, followed by 10 min of incubation at 30°C. 1 mM ATP, 1 mM p[NH]ppA, 2 μM novobiocin, or 100 μg of Oxo per ml was present where indicated. Reactions were incubated for 0.5 min at 30°C with 20–40 ng of pancreatic DNase I (Worthington, DPFF). Exonuclease III (BioLabs) digestions were for 5–15 min at 30°C with 0.05–0.1 unit of nuclease. Reactions were stopped with EDTA, incubated with proteinase K (50 μg/ml) and 0.2% $NaDodSO_4$ for 15 min at 37°C, precipitated with ethanol, and dissolved in 3–10 μl of formamide containing marker dyes (17). The DNA was electrophoresed through a polyacrylamide gel containing 7 M urea or 98% formamide denaturants (17, 18) and autoradiographed.

Abbreviations: bp, base pairs; p[NH]ppA, adenyl-5′-yl imidodiphosphate; Oxo, oxolinic acid.

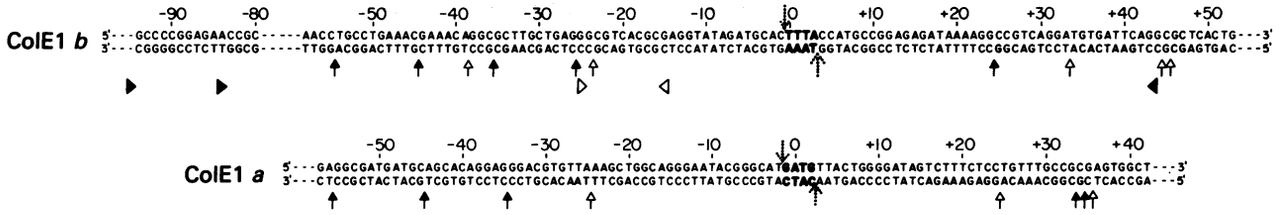

FIG. 1. Nucleotide sequence and summary of nuclease protection of DNA containing the *b* and *a* gyrase sites. The nucleotide sequences around the *b* and *a* sites are numbered about the middle base of the region on the bottom strand that is completely protected from DNase I. The 4 bp within the staggered gyrase cuts (⇣,⇡) are in bold letters. DNase I cuts on the bottom strand are either prominent also in a minus-gyrase control (⇧) or enhanced by gyrase (⇑). Gyrase-specific stalling points for exonuclease III without (▶,◀) or with (▷,◁) p[NH]ppA are shown for the *b* fragment; tips point right or left to indicate the direction of exonucleolysis of the bottom and top strands, respectively.

RESULTS

DNA Sequence at the ColE1 *b* and *a* Gyrase Sites. The *b* and *a* DNA fragments were labeled with ^{32}P at their right (*Mbo* II) termini, and the sequences were determined with the Maxam–Gilbert technique (17). To locate gyrase cuts, the sizes of the fragments after cleavage by gyrase were compared on a denaturing polyacrylamide gel with the DNA generated in the sequence-determination reactions. Because DNA cut by gyrase has a 3′-terminal hydroxyl group, it should migrate more slowly by 1 nucleotide than the corresponding chemically cleaved DNA, which has both 5′- and 3′-terminal phosphates. This 1-base difference was confirmed by using the above *b* and *a* fragments cut with *Hae* III and *Alu* I restriction endonucleases, respectively. The gyrase cut positions on the unlabeled complementary strands were deduced from the known staggering of gyrase cuts. The nucleotide sequences, shown in Fig. 1, are numbered with a base pair between the staggered gyrase cuts set at zero.

Gyrase cut the *a* and *b* sites at these same positions in native ColE1 DNA. The single-stranded 5′ extensions of gyrase-cleaved native ColE1 DNA were repaired with DNA polymerase and combinations of labeled and unlabeled dNTPs as described (8). This data and nearest neighbor analysis gave 5′ T↓G(A,T) and 5′ ↓C(A,T) for the top and bottom strands, respectively, of the *a* site, and 5′ ↓T_n(A) and 5′ ↓T(A_n) for the top and bottom strands, respectively, of the *b* site. (Arrows mark gyrase cuts, additional nucleotides in the repaired ends are in parentheses, and n is 2 or 3.) For both sites, the only sequences near the mapped gyrase cuts consistent with these data and 4-bp staggered cuts are those shown in Fig. 1.

Protection from DNase I at the ColE1 *b* Site. Protection from DNase I was used to analyze gyrase binding to the *b* fragment labeled with ^{32}P at its right end. Incubation with a 2.5-fold molar excess of gyrase and then with competitor DNA results in action of gyrase almost exclusively at the *b* site as determined by the cleavage reaction (12). The DNA was exposed briefly to sufficient DNase I to nick each strand about once on average and was displayed by electrophoresis through a denaturing polyacrylamide gel. Fig. 2*A* shows the result for a control without gyrase (lane 3) and a reaction with enzyme (lane 2). Fragment sizes were calibrated by comparison with chemical cleavages of the same DNA. Cleavage by a small proportion of the gyrase bound at the *b* site resulted in a band at +4 (Fig. 2*A*, lanes 1 and 2), providing a convenient internal calibration marker.

The protection from DNase I is summarized in Fig. 1. The *b* cleavage site was within a central 46-nucleotide region of well-protected DNA, flanked by regions susceptible to DNase I at intervals of about 10 nucleotides. The periodic DNase I cuts are believed to reflect binding of DNA to an exposed protein surface, because this geometry maximally exposes each strand of the duplex to endonuclease at about 10-base intervals (19). Periodic DNase I cuts were at points already prominently cleaved by DNase I [e.g., +34 (Fig. 2*A*)] or were at new, enhanced DNase I sites [e.g., −54 (Fig. 2*B*)]. The region of interaction extended from about −54 to about +50. The same region was entirely protected from digestion by micrococcal nuclease, which makes double-strand breaks. Gyrase binding was not curtailed by proximity of the *b* site to the right end of the *b* frag-

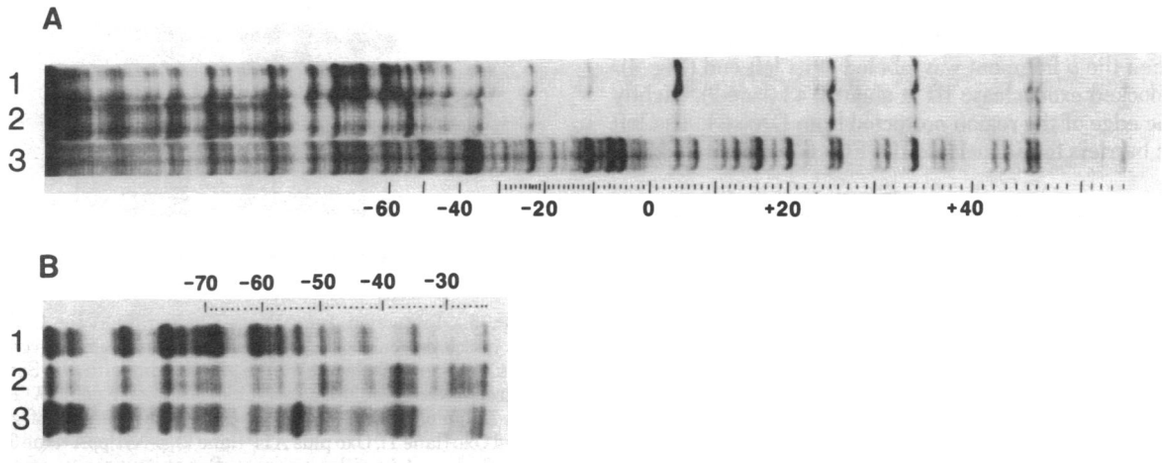

FIG. 2. Protection from DNase I by gyrase at ColE1 *b* site. Reactions contained the *b* fragment labeled with ^{32}P at its right end and were displayed by electrophoresis (from left to right) in acrylamide/urea gels. The scales were derived from reference ladders made by chemical degradation of the *b* fragment by using the Maxam–Gilbert technique. (*A*) Protection from DNase I without gyrase (lane 3), with gyrase (lane 2), and with gyrase plus p[NH]ppA added 1 min after competitor DNA (lane 1). (*B*) Electrophoresis was for a longer time to resolve larger DNA fragments. Lanes: 1, with gyrase and added p[NH]ppA; 2, without gyrase; 3, with gyrase.

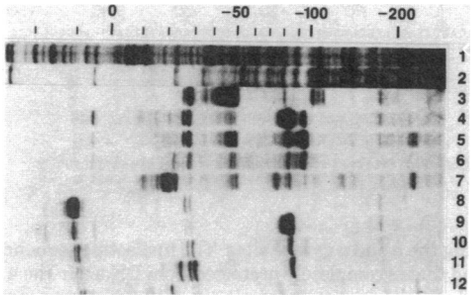

FIG. 3. Use of exonuclease III to define the extreme leftward contacts of gyrase at the ColE1 *b* site. Gyrase reactions containing the *b* fragment labeled at its right terminus were digested with 0.1 unit of exonuclease III for 5 min (lanes 3–7) or 15 min (lanes 8–12). Reactions contained no gyrase (lanes 3 and 8), gyrase (lanes 4 and 9), and gyrase with reagents added 4 min before addition of exonuclease III: Oxo and ATP (lanes 5 and 10); p[NH]ppA (lanes 6 and 11); Oxo and p[NH]ppA (lanes 7 and 12). Protection from DNase I of the same DNA fragment is shown for comparison without gyrase (lane 1) and with gyrase (lane 2). DNA was electrophoresed (from right to left) in an acrylamide/urea gel.

ment because identical results were obtained with a DNA fragment that extends 50 bp further to the right.

Essentially the same pattern of protection from DNase I was observed with topoisomerase II′ bound to the *b* fragment. Topoisomerase II′ is composed of gyrase subunit A and a subunit homologous to part of gyrase subunit B (1). Thus, the nonhomologous portion of subunit B does not influence the DNA wrapping detected by protection from DNase I.

Boundaries of Gyrase Interaction Defined by Exonuclease III. We sought to define the boundaries of the DNA region covered by gyrase by using protection from exonuclease III, which degrades duplex DNA from the 3′ termini. The left extreme of gyrase binding was visualized by using the *b* fragment labeled with ^{32}P at its right end. After a 5-min digestion, gyrase blocked exonuclease III at two specific positions (Fig. 3, lane 4). A higher resolution gel showed these to be essentially unique positions that were mapped at −83 and −94. The more prominent −83 barrier was stable to a 15-min exonuclease III digestion (Fig. 3, lane 9). Strikingly, these exonuclease III barriers lay 30–40 bases outside of the region protected from DNase I (lane 2). The infrequency of DNase I cuts around positions −83 and −94 might have precluded detection of gyrase contacts; however, the DNA between −54 and −80 was clearly exposed to endonuclease.

Exonuclease III invasion from the right terminus was monitored when the *b* fragment was labeled at its left end (Fig. 4). Gyrase blocked exonuclease III at about +43 (lane 2), slightly within the edge of the region protected from DNase I. The left and right barriers to exonuclease III (Fig. 1) show gyrase binding to be asymmetric about the cleavage site.

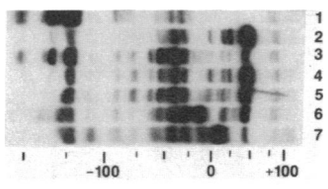

FIG. 4. Right boundary of gyrase binding to ColE1 *b* site as defined by exonuclease III. The *b* fragment, labeled with ^{32}P at its left terminus, was digested for 15 min with 0.05 unit of exonuclease III and electrophoresed (from right to left) in an acrylamide/formamide gel. Reagents were added 4 min before exonuclease III. Lanes: 1, without gyrase; 2, with gyrase; 3, with ATP; 4, with Oxo; 5, with Oxo and ATP; 6, with p[NH]ppA; 7, with Oxo and p[NH]ppA. The scale is derived from size markers consisting of a *Hinf* digest of φX174 DNA.

Conformational Changes of Gyrase. We tested the effects of reagents that alter gyrase conformation on the protection from nucleases by gyrase bound to the *b* fragment. We used: (*i*) ATP, which energizes DNA supercoiling (1); (*ii*) p[NH]ppA, a nonhydrolyzable ATP analogue that allows DNA supercoiling stoichiometric with enzyme amount (13); (*iii*) Oxo, an inhibitor that, if ATP or p[NH]ppA are present, induces about 70% of the gyrase bound at the *b* site to cleave when $NaDodSO_4$ is added (12); (*iv*) novobiocin, a gyrase inhibitor competitive with ATP (13). None of these compounds dramatically altered the DNase I protection pattern (Fig. 5*B*), indicating no gross changes in DNA wrapping.

ATP caused a 30% loss of enzyme from the *b* fragment (measured by retention of DNA to a nitrocellulose filter) and a corresponding loss of protection from DNase I (Fig. 5*B*, lane 7). ATP weakened gyrase barriers to exonuclease III at the right extreme (Fig. 4, lane 3) and left extreme (not shown), but no new barriers were seen. ATP presumably fuels continued Sisyphean cycles of supercoiling of a linear DNA substrate (1). Thus, gyrase conformations other than the one(s) assumed without ATP either must be short-lived or must not have detectable differences in their nuclease protection patterns. The former is more likely because distinctive patterns of protection were seen with p[NH]ppA.

p[NH]ppA caused small but reproducible changes in the protection from DNase I, particularly in the −23 to −54 region (Fig. 2 *A* and *B*, lane 1). Furthermore, a DNase I cut appeared

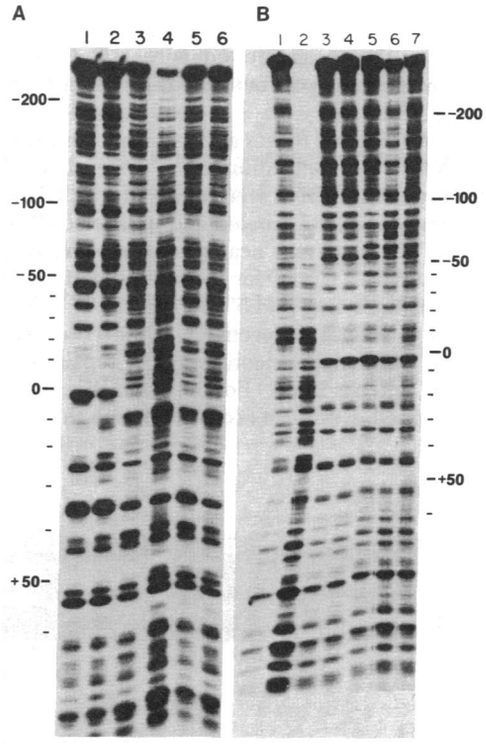

FIG. 5. Protection from DNase I by gyrase at the ColE1 *a* and *b* sites in the presence of ATP and inhibitors. Reactions contained the *a* or *b* fragment labeled at their right termini with ^{32}P. Samples were electrophoresed through acrylamide/formamide gels. (*A*) Fragment *a* with 150 fmol (lanes 1–3) or 250 fmol (lanes 5 and 6) of gyrase with added Oxo (lane 1), Oxo plus ATP (lane 2), p[NH]ppA (lane 3), and ATP (lane 6); lane 4 is without gyrase. Reagents were present from time zero. (*B*) Fragment *b* digested with 40 ng of DNase I, except in lane 1, where digestion was with 20 ng. Lanes: 1 and 2, without gyrase; 3, with gyrase; 4, with Oxo; 5, with Oxo and ATP; 6, with novobiocin; 7, with ATP. Reagents were present from time zero except in lane 5, where ATP was added 1 min before DNase I.

in the central protected region at −11, and cutting between −60 and −85 was enhanced. Novobiocin elicited the same changes (Fig. 5*B*, lane 6). p[NH]ppA destabilized the left −83 barrier (Fig. 3, lanes 6 and 11) and right +43 barrier (Fig. 4, lane 6) to exonuclease III and led to the appearance of new barriers within the central 46-base core region protected from DNase I. Exonuclease III digestion from the left paused at bases clustered at the edge of the central core region (Fig. 3, lanes 6 and 11). Exonuclease III invasion from the right continued through the cleavage site up to a new specific barrier at about −16 (Fig. 4, lane 6). This barrier contained up to 50% of the ^{32}P label in the original +43 barrier and, in time-course experiments, appeared concomitantly with disappearance of the +43 barrier. This implies that, in the presence of p[NH]ppA, the cleavage site is not within the most tightly bound DNA region.

Results with Oxo and p[NH]ppA differed from those with Oxo and ATP (Figs. 3 and 4), although both conditions elicit cleavage at the *b* site. No new specific barriers to exonuclease III were observed with Oxo and ATP, but Oxo and p[NH]ppA elicited new barriers at approximately −20 and +10, enclosing the cleavage site.

Protection from DNase at the ColE1 *a* Site. Protection by gyrase from DNase I was similar at the *a* and *b* sites (Fig. 5). Protection of the *a* fragment, however, required higher levels of gyrase (Fig. 5*A*, lane 5), and was complete only in the presence of Oxo (Fig. 5*A*, lane 1). Cleavage by some of the bound gyrase produced the band at +3 (Fig. 5*A*, lanes 1 and 2). The results are summarized in Fig. 1. Protection from DNase I extended from about −55 to about +40, a slightly shorter region than at the *b* site. ATP and p[NH]ppA reduced protection without specifically altering the pattern (Fig. 5*A*).

Protection of the *a* fragment from exonuclease III absolutely required Oxo; then a stable barrier resistant to high levels of exonuclease III appeared at about −15, far into the region protected from DNase I. A similar barrier was observed at a secondary gyrase cleavage site that was mapped at about −120 in this DNA fragment. Oxo thus appears to strengthen gyrase binding to a small region around the cleavage site.

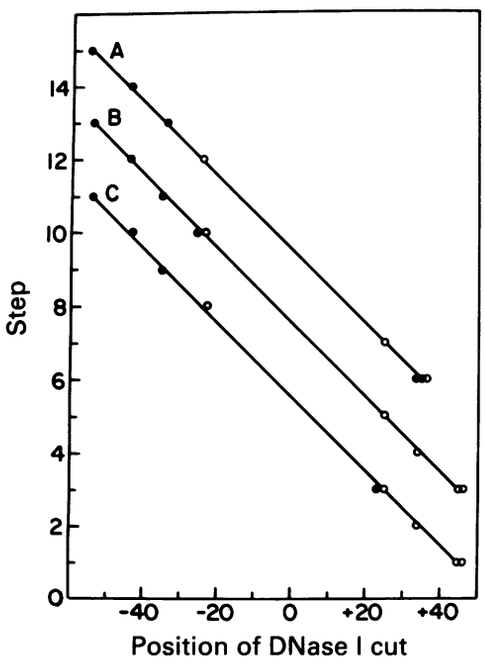

FIG. 6. Periodicity of DNase I cuts of DNA bound by gyrase. To measure the mean periodicity of DNase I-sensitive sites on gyrase-bound DNA, the observed cut positions are plotted (abscissa) against integral steps (ordinate) representing an idealized ladder. ●, Enhanced DNase I cuts; ○, DNase I cuts also prominent in a minus-gyrase control. Lines: A, ColE1 *a* site; B, ColE1 *b* site; C, ColE1 *b* site in presence of p[NH]ppA. The plots are displaced upwards for clarity.

Periodicity of DNase I Cuts. Fig. 6 shows a graphical method of estimating the periodicity of DNase I cuts on gyrase-bound DNA. The observed cut positions are plotted against a ladder of integral steps for the ColE1 *a* site, *b* site, and the *b* site in the presence of p[NH]ppA. Points on either side of the cleavage site fit a straight line, indicating that the DNase I cuts in both flanking regions are in phase. The periodicities of cuts calculated from the slopes were 9.9, 9.9, and 9.8, respectively.

DISCUSSION

Fig. 7 shows how negative supercoiling of DNA might be engineered by gyrase. Fig. 7 step A represents a stable complex between DNA and an $\alpha_2\beta_2$ tetrameric gyrase (1, 10, 20). Consistent with the observed protection from DNase I, DNA is wrapped on the surface of gyrase subunits that are arranged with an axis of 2-fold rotational symmetry through the site of DNA cleavage. Wrapping of the DNA in a right-handed superhelix apposes the "cleaved DNA" segment (shaded) with the "passed DNA" segment (stippled). The entire bound DNA surrounds the cleavage site asymmetrically, consistent with the asymmetry detected by exonuclease III at the *b* site. To effect supercoiling, the passed DNA is transferred through a break in the cleaved DNA (5) by exchange between β protomers (Fig. 7, steps B and C). The specific DNA-binding roles assigned to each subunit are arbitrary but consistent with the division of labor between subunits (1).

Gyrase produces cuts staggered by 4 bp, with each resulting 5′ end attached covalently to an α protomer (8–10). Thus, the cleavage site is placed at a juxtaposition of nucleolytic active sites of α protomers arranged with diad symmetry. This symmetry may be reflected in the protection from DNase I. DNA regions periodically susceptible to DNase I enclosed a protected region whose center was between the staggered gyrase cuts. The precise center is unclear because it appeared to differ by 1 base at the *b* and *a* sites, and the feature recognized by DNase I may lie 1 base from the actual cut (21).

Negative supercoiling by sign inversion requires that gyrase fix the polarity of the passed DNA relative to the cleaved DNA because apposition of these DNA segments with random polarities would lead equally to introduction and removal of negative supertwists (5, 11). The asymmetric cleavage site sequence could allow gyrase to recognize orientation of the cleaved DNA. However, gyrase cannot rely solely on recognition of an asymmetric "passage sequence" to orient a passed DNA segment distant from the cleaved DNA because gyrase negatively supercoils a circular dimer of pBR322 DNAs fused in inverted orientation (22); for each cleavage sequence, this molecule contains two potential passage sequences with opposite polarities. The simplest alternative is that the preferred passed DNA segment is contiguous with the cleaved DNA. Then, the right-handed coiling of DNA around gyrase (Fig. 7) insures that the passed and cleaved DNA segments meet in the proper orientation for negative supercoiling (5). Thus, the exonuclease III barriers at −83 and −94 may detect the relative location of the passed DNA segment. If the DNA wrapping were incomplete, the passed DNA would not necessarily come from DNA adjacent to the cleaved DNA; the two DNA segments would then be connected by DNA of unpredictable writhing or not connected at all. Then the cycle in Fig. 7 could result in DNA supercoiling or relaxation, knotting or unknotting, catenation or decatenation (11).

The periodic DNase I cuts on either side of the *a* and *b* cleav-

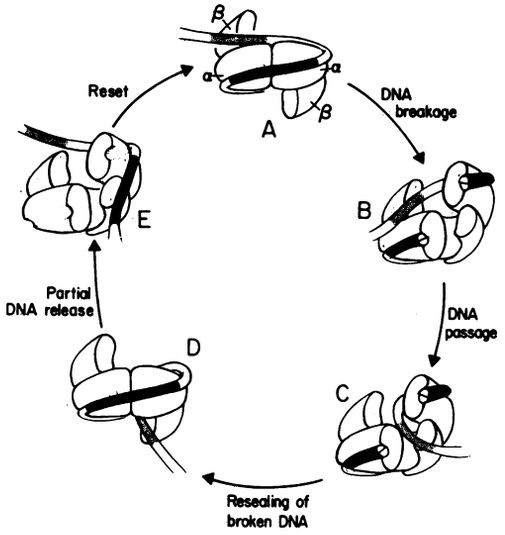

FIG. 7. Model for negative supercoiling of DNA by gyrase. Step A represents a gyrase molecule consisting of two gyrA (α) and two gyrB (β) protomers with a section of a circular duplex DNA (shown as a tube) wrapped in a right-handed superhelix. The shaded DNA, representing the approximately 50-bp central region completely protected from DNase I, contains the site of double-strand breakage at its middle. The stippled DNA, beginning about 85 bp from the cleavage site, is to be passed through the transient gap. The enzyme contains a hole (concealed in step A) that is exposed by opening of the molecule about a hinge between α subunits (as in step B). To effect supercoiling, a right-handed DNA loop in step A is converted into a left-handed one (step D) by the following steps: B, DNA breakage and opening of the enzyme; C, passing of DNA through the gap by exchange of the stippled DNA between β protomers; and D, closing of the enzyme and resealing of the broken DNA. This sequence of steps introduces two negative supercoils. Step E represents a way of resetting the DNA to complete the cycle; the resealed DNA section is released, followed by reopening of gyrase to allow escape of the passed DNA section. A scheme for keying the cycle to the binding and hydrolysis of two ATP molecules follows. With gyrase in the "closed conformation" (steps A or D), interaction of the stippled DNA with a β protomer could allow it to bind an ATP molecule. This in turn could trigger a conformational change—i.e., opening of the gyrase molecule (as in steps B or E). ATP hydrolysis could then stimulate release of DNA from a β protomer and reclosing of gyrase.

age sites were in phase, implying that the DNA is uniformly wrapped by gyrase. However, the observed periodicity of 9.9 is significantly less than the value of 10.6 expected for DNA lying on a flat plane (19). Therefore, the double helix may be overtwisted by 7% upon binding by gyrase. Alternatively, the DNA may lie on a gyrase surface which itself screws left-handedly in space. Thus in Fig. 7 step A, the convex surface of the α protomers rotates by $-180°$ when translated along the DNA axis, thereby reducing the interval of maximum exposure of each strand to 0.5 twists less than the double helical pitch.

The topology of sign inversion, in which gyrase holds both ends of the broken DNA while passing another DNA segment between them, requires the passed DNA to penetrate through a hole in the enzyme (11). This is represented in Fig. 7 step D and must be a feature of all topoisomerases that act by DNA-passing mechanisms. To complete the cycle, the passed DNA could escape from the hole through either its entry port or a separate exit. The latter requires two protein doors that, like lock gates, must not open simultaneously when the DNA is broken at the cleavage site. The alternative of a single entrance/exit requires prior unwrapping of the resealed cleavage site, as shown in Fig. 7 step E. Because gyrase supercoils DNA processively, a strong remaining protein·DNA contact is required, most simply located between the cleaved and passed DNA segments.

Transit of the passed DNA requires opening and closing of the hole in gyrase, described as a flexing of the enzyme normally keyed to ATP binding and hydrolysis (Fig. 7 legend). p[NH]ppA binding allows stoichiometric supercoiling (13) and, thus, can take the cycle through to at least step D of Fig. 7. p[NH]ppA trapped a distinct gyrase conformation at the *b* site, as shown by changes in protection from DNase I and destabilization of the left and right extreme barriers to exonuclease III. Significantly, blockage of exonuclease III digestion from the right at about -16 suggested that the most tightly bound DNA region was left of the cleavage site. We argued above that such an interaction is required if gyrase has only one entry/exit for the passed DNA.

Because nucleotide sequences common to different gyrase binding sites occur only at the cleavage site itself (8), this sequence presumably directs the observed site-specific binding. The "consensus sequence" common to seven sites in ϕX174 and SV40 DNA (11) is 5′ Y-R-T ↓ G-N-Y-N-N-Y (where the arrow marks the gyrase cut in the strand shown, the four bases between the staggered gyrase cuts are underlined, T is preferred for each common pyrimidine (Y) and A for the common purine (R), and N is a random base). Whereas the ColE1 *a* site sequence 5′ C-A-T ↓ G-A-T-G-T-T exactly fits the consensus sequence, the *b* site sequence 5′ C-A-C ↓ T-T-T-A-C-C does not. It lacks the T-G doublet, but has the common purine and 3 pyrimidines appropriately placed.

We thank J. Chou for help with DNA sequence determinations and P. O. Brown and R. J. Otter for purified gyrase. This work was supported by National Institutes of Health Grants GM21397 and CA-19265.

1. Cozzarelli, N. R. (1980) Science **207**, 953–960.
2. Kreuzer, K. N. & Cozzarelli, N. R. (1980) *Cell* **20**, 245–254.
3. Mizuuchi, K., Fisher, L. M., O'Dea, M. H. & Gellert, M. (1980) *Proc. Natl. Acad. Sci. USA* **77**, 1847–1851.
4. Liu, L. F., Liu, C.-C. & Alberts, B. M. (1980) *Cell* **19**, 697–707.
5. Brown, P. O. & Cozzarelli, N. R. (1979) *Science* **206**, 1081–1083.
6. Sugino, A., Peebles, C. L., Kreuzer, K. N. & Cozzarelli, N. R. (1977) *Proc. Natl. Acad. Sci. USA* **74**, 4767–4771.
7. Gellert, M., Mizuuchi, K., O'Dea, M. H., Itoh, T. & Tomizawa, J. (1977) *Proc. Natl. Acad. Sci. USA* **74**, 4772–4776.
8. Morrison, A. & Cozzarelli, N. R. (1979) *Cell* **17**, 175–184.
9. Tse, Y.-C., Kirkegaard, K. & Wang, J. C. (1980) *J. Biol. Chem.* **255**, 5560–5565.
10. Sugino, A., Higgins, N. P. & Cozzarelli, N. R. (1980) *Nucleic Acids Res.* **8**, 3865–3874.
11. Morrison, A., Brown, P. O., Kreuzer, K. N., Otter, R., Gerrard, S. P. & Cozzarelli, N. R. (1980) in *Mechanistic Studies of DNA Replication and Recombination*, eds. Alberts, B. M. & Fox, C. F. (Academic, New York), pp. 785–807.
12. Morrison, A., Higgins, N. P. & Cozzarelli, N. R. (1980) *J. Biol. Chem.* **255**, 2211–2219.
13. Sugino, A., Higgins, N. P., Brown, P. O., Peebles, C. L. & Cozzarelli, N. R. (1978) *Proc. Natl. Acad. Sci. USA* **75**, 4838–4842.
14. Liu, L. F. & Wang, J. C. (1978) *Cell* **15**, 979–984.
15. Liu, L. F. & Wang, J. C. (1978) *Proc. Natl. Acad. Sci. USA* **75**, 2098–2102.
16. Galas, D. J. & Schmitz, A. (1978) *Nucleic Acids Res.* **5**, 3157–3170.
17. Maxam, A. M. & Gilbert, W. (1980) *Methods Enzymol.* **65**, 499–560.
18. Maniatis, T., Jeffrey, A. & van de Sande, M. (1975) *Biochemistry* **14**, 3787–3792.
19. Rhodes, D. & Klug, A. (1980) *Nature (London)* **286**, 573–578.
20. Klevan, L. & Wang, J. C. (1980) *Biochemistry* **19**, 5229–5234.
21. Sollner-Webb, B., Melchior, W. & Felsenfeld, G. (1978) *Cell* **14**, 611–627.
22. Gellert, M., Mizuuchi, K., O'Dea, M. H., Ohmori, H. & Tomizawa, J. (1978) *Cold Spring Harbor Symp. Quant. Biol.* **43**, 35–40.
23. Levitt, M. (1978) *Proc. Natl. Acad. Sci. USA* **75**, 640–644.